ADVANCED MATERIALS

Electroceramics: Characterization by Impedance Spectroscopy

Ferroelectric Ceramics
Grain Boundary Capacitances
Ceramic Electrolytes
Surface Layers on Glasses
Ferromagnetic Ceramics

By John T. S. Irvine,* Derek C. Sinclair,* and Anthony R. West*

Electroceramics are advanced materials whose properties and applications depend on the close control of structure, composition, ceramic texture, dopants and dopant (or defect) distribution. Impedance spectroscopy is a powerful technique for unravelling the complexities of such materials, which functions by utilizing the different frequency dependences of the constituent components for their separation. Thus, electrical inhomogeneities in ceramic electrolytes, electrode/electrolyte interfaces, surface layers on glasses, ferroelectricity, positive temperature coefficient of resistance behavior and even ferrimagnetism can all be probed, successfully, using this technique.

1. Introduction

Electroceramics are high technology materials whose properties and hence, applications depend on a complex interplay of structural, processing and compositional variables. The particular property of interest may be a bulk property of the crystals, in which case, fully dense ceramics free from grain boundary phases are desired. Good examples of this are ceramic electrolytes such as Na β-alumina, $Na_2O.\sim 8Al_2O_3$, used as an $Na^{\oplus}$ ion conducting membrane in Na/S batteries[1] and yttria-stabilized zirconia, $0.9ZrO_2.0.1Y_2O_3$, used as an oxide ion conducting membrane in solid oxide fuel cells and oxygen sensors.[2]

Alternatively, the property of interest may relate specifically to the grain boundaries in polycrystalline materials and perhaps, to differences in behavior between bulk and grain boundary regions. Good examples are varistors, ceramic materials that do not obey Ohm's law.[3] These are usually zinc oxide ceramics in which dopants such as Bi segregate to the grain boundaries. Instead of a linear, I/V, Ohm's law response, the current is given by $I \propto V^a$ where "a" is typically in the range 5–50. Because of the dramatic increase in current with voltage, varistors are used in voltage surge protection devices. Varistor action is far from completely understood but is, undoubtedly, associated with the grain boundary regions of the ceramic.

[*] Prof. A. R. West, Dr. J. T. S. Irvine, Dr. D. C. Sinclair
Department of Chemistry, University of Aberdeen
Meston Building, Meston Walk, Old Aberdeen AB9 2UE (Scotland)

In order to characterize the microstructures and properties of electroceramics, techniques are required that can probe or distinguish between the different regions of a ceramic. Electron microscopy with an analytical facility is, of course, the most direct method for both microstructural characterization and for determining compositional variations within a solid. Corresponding measurements of microscopic electrical properties are possible in principle, as shown by the elegant work of *Dimos* et al. on the effect of grain orientation mismatch on critical current densities in ceramic superconductors.[4] Such measurements with miniature electrodes are not easy, however. Decoration techniques such as cathodoluminescence have been developed for direct observation of grain boundary potential barriers[5]; these permit electrically active grain boundaries to be seen although their properties are not actually measured.

An alternative technique for measuring electrical properties is impedance spectroscopy.[6] In this, AC impedance measurements are made over a wide range of frequencies and the different regions of the material are characterized according to their electrical relaxation times or time constants. Impedance spectroscopy is relatively easy to use and is applicable to a wide variety of materials and problems. It has undergone major developments recently with the availability of automatic equipment capable of spanning many decades of frequency in a single sweep. Long gone are the days of balancing R and C (or L) circuits using null methods, where it could take several minutes to obtain a single reading.

The main purpose of this review is to show the usefulness of impedance spectroscopy for the characterization of electroceramics. It is fast becoming an essential technique in the development of new and improved materials. This is primarily because it enables the overall electrical properties of a material to be separated into their component parts, which can then be systematically studied or modified.

2. Impedance Spectroscopy

2.1. Theory

In impedance spectroscopy, the impedance of a sample is measured over a wide range of frequency, typically 10^{-2} to

  0935-9648/90/0303-0132 $ 02.50/0

ADVANCED MATERIALS

10^7 Hz. Impedances usually have both resistive and reactive (capacitive/inductive) components, both of which must be determined. This can be achieved in various ways; one is to apply an alternating voltage across a sample and a standard resistor which are in series. The in- and out-of-phase components of the voltage across the sample are then measured. Dividing these components by the magnitude of the current gives the resistive and reactive components of the impedance. The measurements are repeated as a step-wise function of frequency.

Different regions of a ceramic sample are characterized by a resistance and a capacitance, usually placed in parallel. The characteristic relaxation time or time constant, τ, of each 'parallel RC element' is given by the product of R and C (Equation 1).

$$\tau = RC \tag{1}$$

$$\omega_{max}\, RC = 1 \tag{2}$$

In the frequency domain, RC elements are separable due to the relation shown in Equation 2 which holds at the frequency of maximum loss, ω_{max}, in the impedance spectrum. From the impedance spectrum, it is therefore usually possible to identify different RC elements and assign them to appropriate regions of the sample. The values of the individual R and C components may then be quantified. Let us now see some practical examples of data and their interpretation.

A common type of impedance spectrum for electroceramics shows the presence of two distinct features attributable to intragrain, or bulk and intergrain, or grain boundary regions. A typical case is shown in Figure 1a for the oxide ion conductor $Ca_{12}Al_{14}O_{33}$.[7] Impedance data are presented in the form of imaginary, Z'' (capacitive) against real, Z' (resistive) impedances. Each parallel RC element (two in Fig. 1) gives rise to a semicircle (ideally) from which the component R and C values may be extracted. R values are obtained from the intercepts on the Z' axis, as shown; C values are obtained by applying Equation 2 to the frequency at the maximum of each semicircle. In this particular case, the two capacitance values are determined to be $\sim 1 \times 10^{-12}$ F and 4×10^{-9} F and the corresponding resistances 0.45 Mohm and 1.15 Mohm.

Having obtained values for these R and C components, the next stage is to assign them to regions of the sample. The assignment is based on the magnitudes of the capacitances (Table 1). For a parallel plate capacitor with area A, separation l between the plates and a medium of permittivity ε' between the plates, the capacitance is given by Equation 3.

$$C = \varepsilon'\, e_0 \frac{A}{l} \tag{3}$$

where e_0 is the permittivity of free space, 8.854×10^{-14} F cm^{-1}. For a material with unit cell constant (i.e. $l/A = 1$ cm^{-1}) and a typical permittivity of ~ 10, a capacitance value of $\sim 1 \times 10^{-12}$ F is expected. Thus, this is a typical value for the bulk capacitance of a sample. The high frequency semicircle in Figure 1 has a capacitance of this

John T. S. Irvine (left) has B.Sc. Chemical Physics (Edinburgh 1981) and Ph.D. (Ulster 1986) degrees. He came to Aberdeen in 1985 where he has been research fellow, Royal Society of Edinburgh Research Fellow and now, Lecturer in chemistry. His Ph.D. topic was on photoelectrochemistry and his research interests have expanded to include high-T_c ceramic superconductors, solid electrolytes and solid state electrochemistry.

Derek C. Sinclair (center) obtained his B.Sc. (1986) and Ph.D. (1989) from Aberdeen University and is currently a Research Fellow in the Chemistry Department. His Ph.D. topic was on the characterization of electroceramics and he is currently researching into high-T_c superconductors.

Anthony R. West (right) has B.Sc. (Wales 1968), Ph.D. (Aberdeen 1971) and D.Sc. (Aberdeen 1984) degrees. He has been, successively, Lecturer, Senior Lecturer and Reader in chemistry and in 1989 was appointed to a personal professorship in Aberdeen. His research covers many aspects of solid state chemistry and ceramics, and he is author of about 180 research publications and the books 'Solid State Chemistry and its Applications' and 'Basic Solid State Chemistry'.

  0935-9648/90/0303-0133 $ 02.50/0

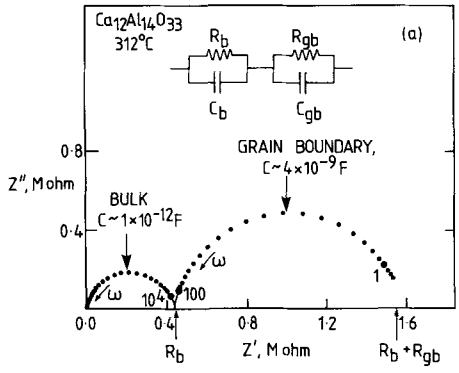

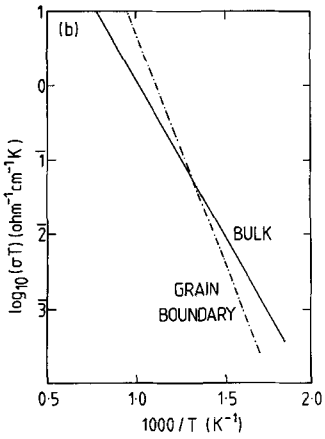

Fig. 1. a) Impedance data for $Ca_{12}Al_{14}O_{33}$ presented in the complex impedance plane format, Z'' vs Z' where $Z^* = Z' - jZ''$, $j = \sqrt{-1}$, ω = angular frequency $2\pi f$. Selected frequency points, in Hz are marked. The equivalent circuit used to interpret the data is shown. It represents a series combination of crystal and grain boundary impedances. b) Temperature dependence of bulk and grain boundary conductivities for $Ca_{12}Al_{14}O_{33}$.

order and therefore, this semicircle and its associated resistance is attributed to the bulk properties of the sample.

Table 1. Capacitance values and their possible interpretation.

Capacitance [F]	Phenomenon Responsible
10^{-12}	bulk
10^{-11}	minor, second phase
10^{-11}–10^{-8}	grain boundary
10^{-10}–10^{-9}	bulk ferroelectric
10^{-9}–10^{-7}	surface layer
10^{-7}–10^{-5}	sample-electrode interface
10^{-4}	electrochemical reactions

In order to assign the second semicircle to a feature of the ceramic, it is essential to have a picture of an idealized ceramic with grains and grain boundaries and consider the factors which control the magnitude of the grain boundary impedance. The 'brickwork' model shown in Figure 2 represents a ceramic composed of cube-shaped grains of dimensions l_1, separated from each other by a boundary of thickness l_2. For this idealized case, Equation 4 holds. This arises

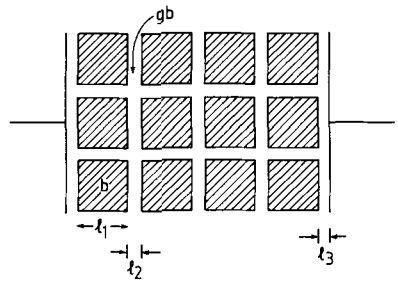

Fig. 2. Brickwork model of grain and grain boundary regions in a ceramic placed between metal electrodes.

from the inverse relation between thickness and capacitance given by Equation 3. A wide variety of ceramic microstructures occur in practice and it is found that the grain boundary capacitance usually lies in the range 10^{-11} to 10^{-8} F; the higher capacitances occur in materials that are

$$\frac{C_b}{C_{gb}} = \frac{l_2}{l_1} \tag{4}$$

well-sintered, with narrow intergranular regions. The lower capacitances are often found with poorly sintered samples that contain constriction resistances or narrow contacting 'necks', between grains.[81] For the case in Figure 1, the grain boundary capacitance is quite large, indicating a well-sintered sample. Nevertheless, the overall resistance of these narrow grain boundaries is 2–3 times greater than the resistance of the grains.

2.2. Applications

Results such as those shown in Fig. 1a are useful for several reasons:

- to indicate whether the overall resistance of a material is dominated by bulk or grain boundary components
- to assess the quality and electrical homogeneity of an electroceramic, since there is generally a link between sintering/microstructure and AC response
- to measure the values of the component resistances and capacitances.

The temperature dependence of resistance is usually plotted in Arrhenius format, as shown in Figure 1b for the $Ca_{12}Al_{14}O_{33}$ sample.

Bulk and grain boundary effects are only two of a number of effects that can be studied by impedance spectroscopy. Some of these are listed in Table 1 and are characterized by their relative capacitance values. The distinction between components is usually fairly straightforward unless the material contains a ferroelectric component, with a typical bulk permittivity in the range 10^3 to 10^5. In such cases, however, ferroelectric components are usually distinguishable from non-ferroelectric thin layer effects by the temperature dependence of their capacitances, as discussed later.

0935-9648/90/0303-0134 $ 02.50/0

ADVANCED MATERIALS

Surface layers are often found on electroceramics; a good example is provided by lithium silicate glass.[9] Although this transparent glass is apparently atmosphere-stable and water-insoluble, it does in fact form a hydrated/carbonated surface layer very quickly during cooling of the melt. This shows up in the impedance spectrum, Figure 3a, as an additional, poorly-resolved semicircle. A glass without this layer, Fig. 3b, shows only one semicircle, corresponding to lithium ion conduction through the bulk of the glass and a nearly vertical, low frequency 'spike' representing charge build-up at the blocking metal electrodes. Using impedance spectroscopy, it is possible to study the conditions for formation/removal of the surface layer and the associated kinetics.

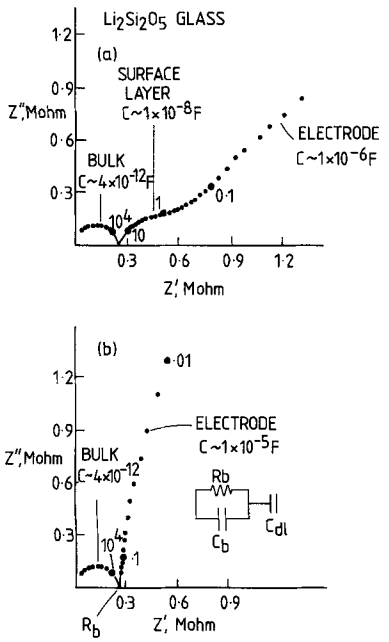

Fig. 3. Impedance data for a lithium silicate glass (a) with, and (b) without the presence of a surface layer caused by atmospheric attack. Both data sets recorded at 130 °C.

The interface between sample and electrode is important for various reasons. One is that the impedance response can give information on the nature of the conducting species within the ceramic and in particular, whether conduction is by ions or electrons. Two different examples are shown in Figure 4. In (a), data for $LiGaSiO_4$ ceramic with metal electrodes take the form of a single semicircle with a capacitance of 2×10^{-12} F.[10] This may be interpreted in terms of the bulk response of the sample and a single parallel *RC* element. There is no sign in the data of a low frequency 'electrode spike'. It was concluded, therefore, that there was no impedance barrier to charge transfer between the metal electrode and the ceramic and that the conducting species were electrons.

The opposite extreme arises when the sample-electrode interface is purely capacitive and no charge transfer occurs across the interface; a good example of this is lithium silicate glass with metal electrodes (Fig. 3b).

For the other example shown in Figures 4a and 4b, the electrode-sample interface is partially blocking. The sample

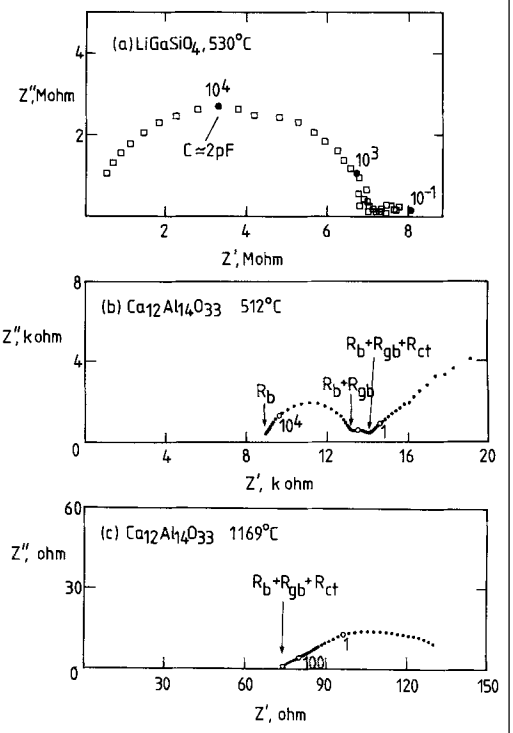

Fig. 4. Impedance data for (a) electronically conducting $LiGaSiO_4$ and (b, c) $Ca_{12}Al_{14}O_{33}$, an oxide ion conductor.

is again $Ca_{12}Al_{14}O_{33}$, as in Figure 1. This time, the impedance data are recorded at higher temperatures. Consequently, the semicircle corresponding to the bulk impedance is out with respect to the frequency scale of the instrumentation in both (b) and (c); the grain boundary semicircle is off scale in (c). In (b), three features are seen. The large semicircle corresponds to the grain boundary impedance, as in Figure 1. The small, poorly resolved semicircle has an associated capacitance of 2.2×10^{-6} F and is associated with electron transfer to and from the oxide ions at the electrode-ceramic interface. The value of the associated charge transfer resistance may therefore be determined. The low frequency spike inclined at 45° is associated with diffusion of oxygen molecules through the electrode.

At higher temperatures (Fig. 4c) the charge transfer component becomes negligible and the inclined spike turns over in the form of a semicircle, indicating that the diffusion is through a layer of finite thickness.

Results such as these are strongly indicative of the nature of the conducting species, therefore. They can also be used to monitor the kinetics of gas-solid reactions. Important areas of study are the redox reactions occurring at the electrodes in fuel cells, sensors and some catalysts.

  0935-9648/90/0303-0135 $ 02.50/0

2.3. Data Processing

Most of the examples so far have been of ionically conducting ceramics in which the complex impedance plane representation, Z'' vs Z', is an appropriate method for presenting the results. It is often the case, however, that alternative formalisms of data presentation can yield additional information that is not easily accessible from the impedance plane alone. Semiconducting ceramics such as donor-doped, ferroelectric $BaTiO_3$ are a case in point.[11] These are electrically inhomogeneous materials in which the grain boundary resistance may, in certain circumstances, dominate the overall impedance. A single semicircle is then seen in the complex impedance plane (Fig. 5a) which does in fact show a slight departure from ideality at high frequencies. If the same data are reprocessed and presented in the complex electric modulus, M^*, formalism (Equation 5) where $j = \sqrt{-1}$, $\omega =$

$$M^* = j\omega C_0 Z^* \tag{5}$$

angular frequency $2\pi f$ and $C_0 = e_0 A/l$, then the response of both grain boundary and bulk regions may be seen. This is demonstrated most clearly in the form of spectroscopic plots of the imaginary components M'' and Z'' (Fig. 5b). The Z'' plot contains a single peak, corresponding to the semicircle in Figure 5a but the M'' plot shows two peaks. The higher frequency M'' peak represents a bulk component of the sample.

The value of presenting data as both M'' and Z'' spectroscopic plots is that they give different weightings to the data and therefore, highlight different features of the sample. Thus, impedance plots pick out the most resistive elements in the sample, since the impedance peak height, Z''_{max}, is equal to $R/2$ for that particular element. Modulus plots pick out those elements with the smallest capacitance since the M'' peak maximum is equal to $e_0/2C$ for that particular element. In materials that are inhomogeneous and are represented by more than one RC element, the resulting M'' and Z'' spectra may look very different (as in Fig. 5b).

Plots such as Figure 5b have been invaluable for characterizing barium titanate devices that show the PTCR (positive temperature coefficient of resistance) effect; such devices are used in current overload protection devices. In particular, it has been possible to separate the ferroelectric and non-ferroelectric components of an electrically inhomogeneous material, by recording the temperature dependence of the capacitances (Fig. 5c). Capacitance C_1 is temperature independent and pertains to the non-ferroelectric grain boundaries. Capacitance C_2 shows a very marked temperature dependence, increasing asymptotically towards the Curie temperature, T_c. It is therefore characteristic of a ferroelectric material that is above the Curie temperature. This

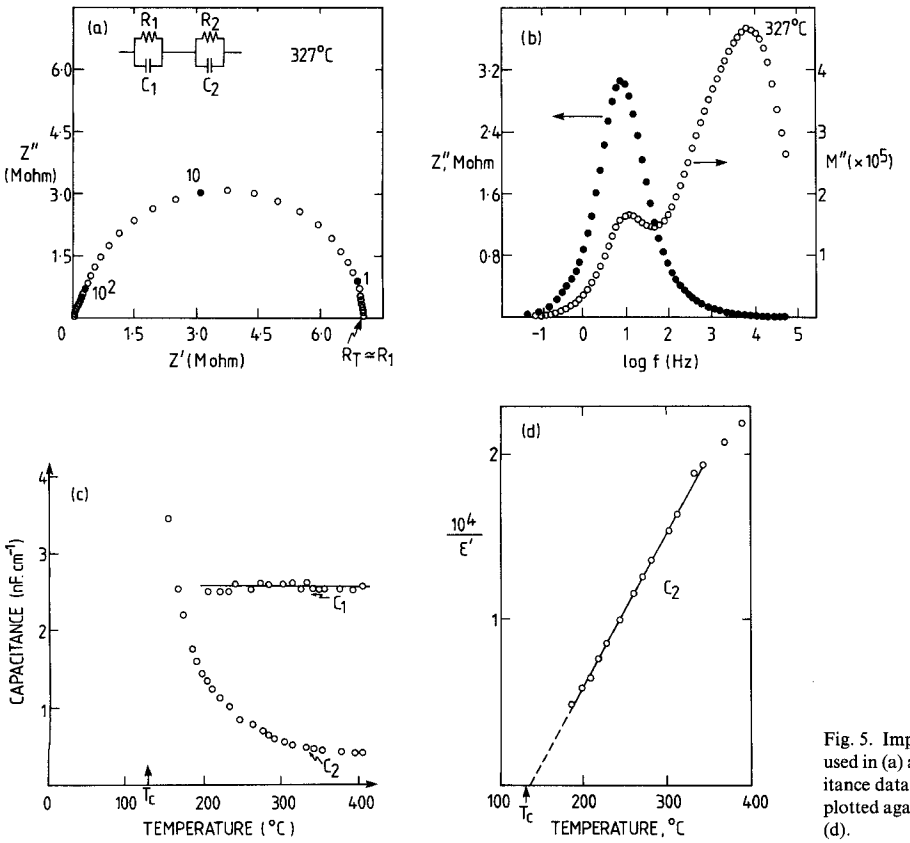

Fig. 5. Impedance data for doped $BaTiO_3$. The same data are used in (a) and (b) but are presented in different ways. Capacitance data obtained from M'' peaks such as shown in (b) are plotted against temperature in (c) and as a Curie-Weiss plot in (d).

0935-9648/90/0303-0136 $ 02.50/0

ADVANCED MATERIALS

is confirmed by presenting the data as a Curie-Weiss plot of reciprocal capacitance against temperature (Fig. 5d).

3. Single Crystal Studies

Studies on single crystal materials have the advantage that grain boundary phenomena should be absent and a more detailed analysis of bulk properties may be made. A good example is $LiTaO_3$, a ferroelectric material used for its non-linear optical properties. Impedance spectroscopy has allowed a detailed breakdown of its electrical properties, as a function of crystallographic orientation.[12] The equivalent circuits which were found to fit the data for the two crystal orientations with the electric field parallel and perpendicular to the polar c axis, are shown in Figure 6(a, b) respectively. The temperature dependence of the component C and R values are shown in Figures 6c and 6d for the parallel orientation and in Figure 6e for the perpendicular orientation. In the ferroelectric orientation (6a), at temperatures below the Curie point, $\sim 590\,^{\circ}C$, the AC response of the sample indicates the presence of five components:

(i) Capacitance C_1, corresponding to the overall permittivity of the sample. This is characteristic of the ferroelectric state below T_c; it passes through a sharp maximum at T_c (Fig. 6c).

(ii) Resistance R_1, in series with capacitance C_1. This represents the resistance to reversal or switching of the ferroelectric domains. With increasing temperature, R_1 decreases more rapidly, with pronounced curvature towards T_c (Fig. 6d).

(iii) Capacitance C_2 in parallel with resistance R_1. This represents the bulk polarization of the lattice and is largely independent of the ferroelectric domain structure. Its value is large for a bulk component, 10^{-9}–10^{-10} F, and is essentially temperature independent but shows a small increase on passing through T_c.

(iv) Resistance R_2 in parallel with the other three elements R_1, C_1 and C_2. This represents the leakage resistance of the crystal which, in this crystallographic orientation is caused by migration of lithium ions. It gives a linear Arrhenius plot (Fig. 6d).

(v) Capacitance C_3, in series with the other four elements of the equivalent circuit. It corresponds to formation of a double layer at the crystal-electrode interface since the gold electrodes are blocking transport of $Li^{\oplus}$ ions. Its value, $\sim 2 \times 10^{-6}$ F, is a typical double layer value.

These results (i–v) represent a major advance over the analyses that were previously possible, which were essentially confined to measurements of the overall permittivity as a function of temperature (Fig. 6c).

In the non-ferroelectric orientation (Fig. 6b, e) the impedance response is very simple. The sample is predominantly a

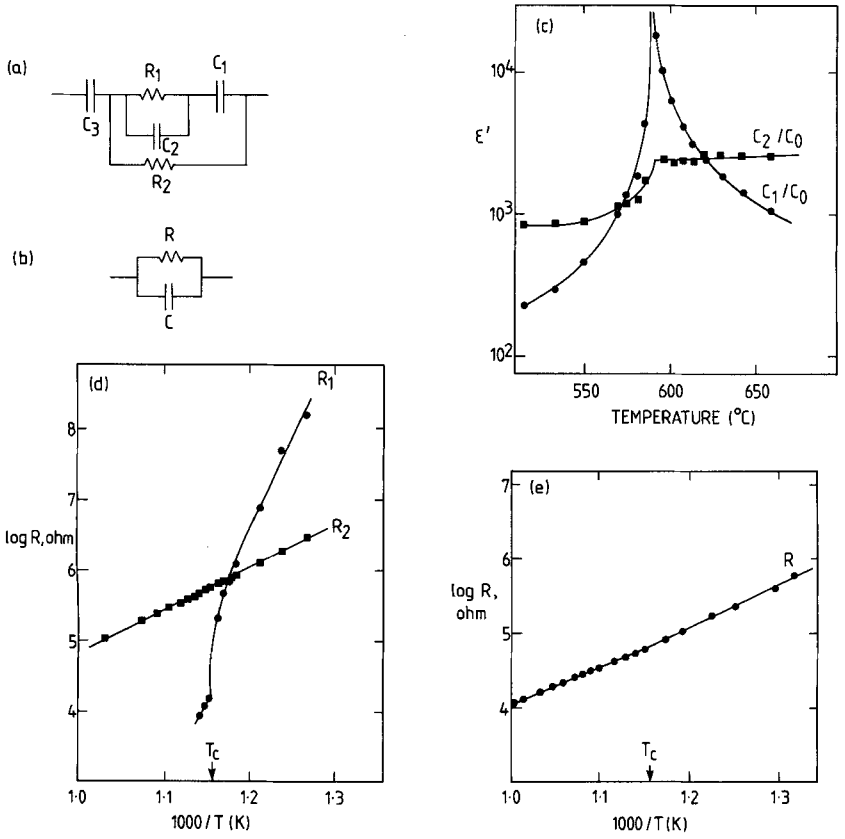

Fig. 6. Impedance data for $LiTaO_3$ single crystal. (a, b) equivalent circuits for voltage applied parallel and perpendicular to polar c axis, respectively. (c, d) C and R data for orientation (a). (e) R data for orientation (b).

  0935-9648/90/0303-0137 $ 02.50/0

poor electronic semiconductor. The parallel capacitance value, $\sim 1 \times 10^{-12}$ F, is typical of that for a non-ferroelectric solid. The AC response is represented by a single *RC* element therefore and the resistance gives a linear Arrhenius plot.

The results obtained in the ferroelectric orientation provide, for the first time, a ready means of quantifying the difficulty of domain reorganization, in terms of the parameter R_1. Since reversal of ferroelectric domains can be monitored by impedance spectroscopy, it seemed highly likely that, with appropriate measurements, magnetic domain reorganization could also be studied. This was indeed shown to be the case with a Ni, Zn ferrite ceramic sample.[13]

Results are shown in Figure 7 for the ferrite placed inside a coil of Cu wire. The AC response of the coil was measured and analyzed to give information on the resistive and inductive properties of the ferrite. The equivalent circuit used to model the data is shown in Figure 7a and the temperature dependences of the *R*, *L* components in Figure 7b and 7c. There are clearly two components to the overall inductance of the sample, both of which have a maximum value just below the Curie point. The associated resistances again represent the resistance to domain reorganization and show a characteristic, nonlinear decrease to zero at the Curie temperature.

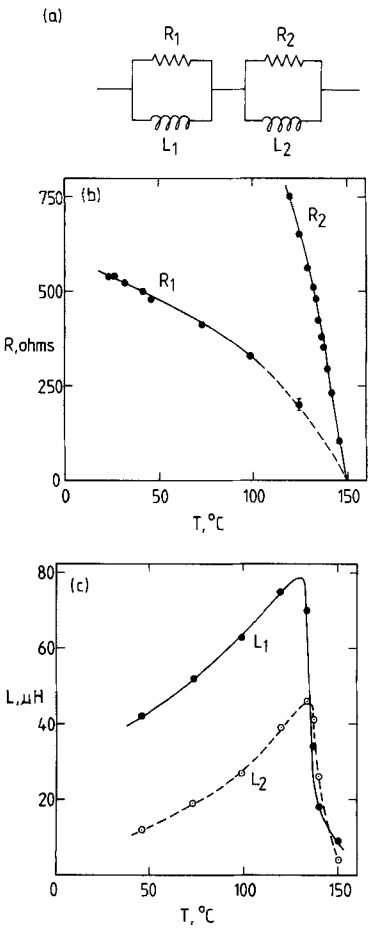

Fig. 7. Magnetic impedance data for a Ni, Zn ferrite showing (a) equivalent circuit (b) temperature dependence of resistances, (c) temperature dependence of inductances.

Work on the characterization of such magnetic phenomena has only just commenced but it is already clear that a wealth of information may be obtained by impedance spectroscopy. Future developments are likely to involve the separation and characterization of resonance/relaxation phenomena and the separation of these reversible effects from irreversible effects associated with hysteresis at high magnetic fields.

4. Conclusions

This overview of impedance spectroscopy chooses various examples, taken from our laboratory, which illustrate the power and usefulness of the technique for characterizing a wide variety of materials and phenomena. Sometimes, the properties that are measured are of prime concern, as for instance, the bulk resistance of oxide ion conductors. In other cases, we use the fact that materials have measurable electrical properties to allow us to study other phenomena such as corrosion or catalysis.

Received: October 5, 1989

[1] J. L. Sudworth, A. R. Tilley: *The Sodium-Sulfur Battery*, Chapman and Hall, London 1985.
[2] T. Takahashi: *High Conductivity Solid Ionic Conductors*, World Scientific, Singapore 1989.
[3] G. D. Mahan, L. M. Levinson, H. R. Phillipp, *J. Appl. Phys. 50* (1979) 2799.
[4] D. Dimos, P. Chaudhari, J. Mannhart, F. K. LeGoues, *Phys. Rev. Lett. 61* (1988) 219.
[5] H. Ihrig, M. Klerk, *Appl. Phys. Lett. 35* (1979) 307.
[6] J. Ross Macdonald: *Impedance Spectroscopy*, Wiley, Chichester 1987.
[7] J. T. S. Irvine, M. Lacerda, A. R. West, *Mat. Res. Bull. 23* (1988) 1033.
[8] P. G. Bruce, A. R. West, *J. Electrochem. Soc. 30* (1983) 662.
[9] W. B. Reid, A. R. West, *Solid State Ionics 28–30* (1988) 681.
[10] P. Quintana, A. R. West, *Solid State Ionics 23* (1987) 179.
[11] D. C. Sinclair, A. R. West, *J. Appl. Phys. 66* (1989) 3850.
[12] D. C. Sinclair, A. R. West, *Phys. Rev. B 39* (1989) 13486.
[13] J. T. S. Irvine, A. Huanosta, E. Amano, R. Valenzuela, A. R. West unpublished results.

0935-9648/90/0303-0138 $ 02.50/0